

Citation for published version:

Speck, T & Jack, RL 2016, 'Ideal bulk pressure of active Brownian particles', *Physical Review E*, vol. 93, no. 6, 062605. <https://doi.org/10.1103/PhysRevE.93.062605>

DOI:

[10.1103/PhysRevE.93.062605](https://doi.org/10.1103/PhysRevE.93.062605)

Publication date:

2016

Document Version

Publisher's PDF, also known as Version of record

[Link to publication](#)

University of Bath

Alternative formats

If you require this document in an alternative format, please contact:
openaccess@bath.ac.uk

General rights

Copyright and moral rights for the publications made accessible in the public portal are retained by the authors and/or other copyright owners and it is a condition of accessing publications that users recognise and abide by the legal requirements associated with these rights.

Take down policy

If you believe that this document breaches copyright please contact us providing details, and we will remove access to the work immediately and investigate your claim.

Ideal bulk pressure of active Brownian particles

Thomas Speck¹ and Robert L. Jack²

¹*Institut für Physik, Johannes Gutenberg-Universität Mainz, Staudingerweg 7-9, 55128 Mainz, Germany*

²*Department of Physics, University of Bath, Bath BA2 7AY, United Kingdom*

(Received 1 December 2015; published 10 June 2016)

The extent to which active matter might be described by effective equilibrium concepts like temperature and pressure is currently being discussed intensely. Here, we study the simplest model, an ideal gas of noninteracting active Brownian particles. While the mechanical pressure exerted onto confining walls has been linked to correlations between particles' positions and their orientations, we show that these correlations are entirely controlled by boundary effects. We also consider a definition of local pressure, which describes interparticle forces in terms of momentum exchange between different regions of the system. We present three pieces of analytical evidence which indicate that such a local pressure exists, and we show that its bulk value differs from the mechanical pressure exerted on the walls of the system. We attribute this difference to the fact that the local pressure in the bulk does not depend on boundary effects, contrary to the mechanical pressure. We carefully examine these boundary effects using a channel geometry, and we show a virial formula for the pressure correctly predicts the mechanical pressure even in finite channels. However, this result no longer holds in more complex geometries, as exemplified for a channel that includes circular obstacles.

DOI: [10.1103/PhysRevE.93.062605](https://doi.org/10.1103/PhysRevE.93.062605)

I. INTRODUCTION

Thermal equilibrium is quite special, not the least because the same quantity, the free energy, determines the probabilities of fluctuations and the work for reversible changes [1]. As one consequence, in thermal equilibrium, the *mechanical* pressure exerted by a fluid on its confining walls is equal to a derivative of the free energy. Moreover, pressure is an intensive quantity and is constant throughout a large system. These properties are often taken for granted and have profoundly shaped our physical intuition.

This intuition is challenged in nonequilibrium systems, where a mechanical pressure may still be measured from the forces exerted on confining walls, but is no longer calculable from a free energy. A fundamental question is whether the pressure in such a system can be related to its bulk properties, through an equation of state. This question has received considerable attention recently for active Brownian particles (ABPs) [2–12]. ABPs are driven out of equilibrium due to directed motion at a constant effective force, the direction of which undergoes rotational diffusion. This model is conceptually simple, but still captures essential properties of active matter. In particular, interacting ABPs show a motility-induced phase transition strongly resembling passive liquid-gas separation but caused dynamically [13–20]. Due to their persistence of motion, ABPs accumulate at walls [21–23] and exert a force, viz., a pressure, the properties of which have been studied for several geometries [24–30]. The sedimentation profile of ABPs [31,32] also enables the discussion of pressure in experiments [33]. Several works have conjectured that an *equation of state* exists for ABPs, relating the mechanical pressure (in infinite systems) to bulk properties [2,5,9]. Recently, Falasco *et al.* have derived an equation of state that explicitly includes the dissipation [34].

The main purpose of this article is to highlight the distinction between the mechanical pressure p_{wall} and the *local* pressure p_{loc} , which is calculated in an open subsystem, due to forces exerted by its surroundings. Both the mechanical

pressure and the local pressure can also be expressed in terms of a *virial* pressure. Our central result is that for ideal ABPs, the local pressure is still given by the equilibrium formula $p_{\text{loc}}(\mathbf{r}) = \rho(\mathbf{r})T$ (with local density ρ and Boltzmann's constant set to unity), independent of the driving. This might seem surprising because the mechanical pressure clearly depends on the active forces.

We give several arguments as to why the local pressure is nevertheless a useful concept giving deeper insights into the nature of active matter. In particular, it relates to the existence of an equation of state for ABPs, for which we consider two formulations. The weak formulation states that the mechanical pressure can be predicted from the measurement of some properties (to be specified) far away from any confining walls onto which the pressure is exerted. This interpretation is followed, e.g., by Solon *et al.* in Ref. [5]. In a stronger formulation, we further demand that the mechanical pressure is directly related to forces that act in the bulk, and hence to the local pressure. Only in this case does one recover the properties commonly associated with the thermodynamic pressure, as becomes evident from the fact that the equation of state does not predict the observed phase boundaries [5], and the existence of a negative interfacial tension [8]. This distinction between mechanical pressure and local pressure is also of practical importance since the equivalence of local and mechanical pressure underpins the use of equilibrium statistical mechanics and numerical simulations to predict the mechanical pressure from atomistic simulations employing periodic boundary conditions, which is indeed one of the first applications of modern computing machines [35].

This article is organized as follows. In Sec. II, we introduce the model of noninteracting ABPs and derive the virial pressure in a large closed system following previous results. In Sec. III, we present three analytical pieces of evidence for a local pressure based on the Smoluchowski equation with explicit (although infinitely separated) walls. We then consider finite wall separations in Sec. IV showing that mechanical and virial pressure still coincide if treating the boundary conditions

correctly. In Sec. V, we discuss the implications of our results, before concluding.

II. MODEL AND VIRIAL PRESSURE

A. Active ideal gas

We consider an ideal (noninteracting) system of N active Brownian particles in two dimensions. Each particle has a position \mathbf{r} and an orientation \mathbf{e} . Particle i moves according to the Langevin equation $\dot{\mathbf{r}}_i = \mu_0 \mathbf{F}_i$ where μ_0 is a (bare) mobility, and the total force on particle i is

$$\mathbf{F}_i = \mathbf{F}_i^s + (v_0/\mu_0)\mathbf{e}_i + \boldsymbol{\xi}_i, \quad (1)$$

in which the forces \mathbf{F}_i^s come from confining walls (which may be hard or “soft”), v_0 is the speed of the active motion, and $\boldsymbol{\xi}_i$ is a thermal noise with correlations

$$\langle \xi_i^\alpha(t) \xi_j^\beta(t') \rangle = (2T/\mu_0) \delta_{ij} \delta^{\alpha\beta} \delta(t - t'), \quad (2)$$

where α, β label vector components. Throughout, we set Boltzmann’s constant to unity. The temperature T determines the translational diffusion while the evolution of the orientations is decoupled and independent of temperature. We consider a two-dimensional box of size $L \times L_y$. For results that are also valid in three dimensions, we use $d = 2$ as placeholder for the dimensionality.

B. Virial pressure for closed systems

A standard route to calculate the pressure is the virial

$$W \equiv \sum_{i=1}^N \langle \mathbf{F}_i \cdot \mathbf{r}_i \rangle = \sum_i \left[\langle \mathbf{F}_i^s \cdot \mathbf{r}_i \rangle + (v_0/\mu_0) \langle \mathbf{e}_i \cdot \mathbf{r}_i \rangle \right]. \quad (3)$$

We use the Itô convention so $\langle \boldsymbol{\xi}_i \cdot \mathbf{r}_i \rangle = 0$. Additionally, $\partial_t \langle |\mathbf{r}_i|^2 \rangle = 0$ holds in the steady state of the system and Itô’s formula yields $\sum_i \langle \dot{\mathbf{r}}_i \cdot \mathbf{r}_i \rangle + NT\mu_0 d = 0$. Hence, from $\mathbf{F}_i = \dot{\mathbf{r}}_i/\mu_0$ we find $W = -NTd$.

The first term on the right-hand side of Eq. (3) arises from interactions of particles with the confining walls. The classical argument [36] assumes a pressure p_{wall} that is isotropic and equal on all walls, and considers these walls one at a time. We place the origin in the lower left corner of the box and consider forces from the wall at $x = L$: the average total force from that wall $\sum_i \langle \mathbf{F}_i^s \rangle_L$ points along the $(-x)$ direction with magnitude $p_{\text{wall}} L_y$. All particles that interact with the wall have $x \approx L$ so this wall contributes $-p_{\text{wall}} L L_y$ to the virial. The wall at $y = L_y$ gives an identical contribution. Combining these results and using the fact that particles evolve independently predicts that the wall pressure is given by the virial pressure,

$$p_{\text{wall}} = p_{\text{vir}}^{\text{closed}} \equiv \bar{\rho} T + \frac{v_0 \bar{\rho}}{\mu_0 d} \langle \mathbf{e}_i \cdot \mathbf{r}_i \rangle, \quad (4)$$

where $\bar{\rho} \equiv N/(LL_y)$ is the average density. For a diffusive ideal gas ($v_0 = 0$) we recover the ideal gas law $p_{\text{wall}} = \bar{\rho} T$. In general, notice that Eq. (4) is a relation between the pressure at the walls and the average density in a closed system.

C. Freely diffusing orientations

The derivation of Eq. (4) made no assumptions about the dynamical evolution of the orientation \mathbf{e} . In the simplest ABP

model, we assume that this vector undergoes free rotational diffusion with correlation time τ_r , so that

$$\langle \mathbf{e}(t) \cdot \mathbf{e}(t') \rangle = e^{-|t-t'|/\tau_r} \quad (5)$$

and the stochastic dynamics of the system is Markovian.

In two dimensions ($d = 2$), we write the particle orientation as $\mathbf{e} = (\cos \varphi, \sin \varphi)^T$. The time evolution of the joint probability $\psi(\mathbf{r}, \varphi, t)$ of the position and orientation of a single particle is then governed by

$$\partial_t \psi = -\nabla \cdot [v_0 \mathbf{e} + \mu_0 \mathbf{F}^s] \psi + \frac{1}{\tau_r} \partial_\varphi^2 \psi + \mu_0 T \nabla^2 \psi. \quad (6)$$

Since particles are independent, this equation fully describes our system: the normalization of ψ is $\int d\mathbf{r} \int d\varphi \psi(x, \varphi) = N$. In the following, it will be convenient to define the local density

$$\rho(\mathbf{r}) \equiv \int_0^{2\pi} d\varphi \psi(\mathbf{r}, \varphi) \quad (7)$$

and the local polarization density

$$\mathbf{p}(\mathbf{r}) \equiv \int_0^{2\pi} d\varphi \mathbf{e} \psi(\mathbf{r}, \varphi) \quad (8)$$

of the fluid.

D. Virial pressure for a large closed system

As a first step, from Eqs. (4) and (6) we calculate the mechanical pressure in a large confined system. To this end, we consider the correlation function

$$c(t) \equiv \langle \mathbf{e}_i(t) \cdot \mathbf{r}_i(t) \rangle = \int d\mathbf{r} \int_0^{2\pi} d\varphi (\mathbf{e} \cdot \mathbf{r}) \psi(\mathbf{r}, \varphi, t). \quad (9)$$

The \mathbf{r} integral runs over the entire x, y plane. The system is confined by the walls so $\psi \rightarrow 0$ as $|\mathbf{r}| \rightarrow \infty$. The equation of motion for this correlation function is

$$\partial_t c(t) = \int d\mathbf{r} \int_0^{2\pi} d\varphi (\mathbf{e} \cdot \mathbf{r}) \partial_t \psi(\mathbf{r}, \varphi, t). \quad (10)$$

Using Eq. (6) and integration by parts yields

$$\partial_t c(t) = \int d\mathbf{r} \int_0^{2\pi} d\varphi \psi \left[(v_0 \mathbf{e} + \mu_0 \mathbf{F}^s) \cdot \nabla (\mathbf{e} \cdot \mathbf{r}) + \frac{1}{\tau_r} \partial_\varphi^2 (\mathbf{e} \cdot \mathbf{r}) \right]. \quad (11)$$

There are no boundary terms because $\psi \rightarrow 0$ at large distances, and the integrand is periodic in φ . Evaluating the derivatives yields $\partial_t c(t) = \langle v_0 (\mathbf{e} \cdot \mathbf{e}) + \mu_0 (\mathbf{e} \cdot \mathbf{F}^s) \rangle - c(t)/\tau_r$. In a large system, the fraction of time that any particle spends in contact with the wall vanishes, so $\langle \mathbf{e} \cdot \mathbf{F}^s \rangle \rightarrow 0$. Hence, in steady state one has $c(t) = v_0 \tau_r \equiv \ell_p$ independent of t . The directed motion is characterized by the persistence length ℓ_p , which is the typical length over which particle orientations persist. Plugging this result into Eq. (4) yields [2–10]

$$p_{\text{wall}}(\bar{\rho}, T, v_0) = \bar{\rho} T + p_0, \quad p_0 \equiv \frac{v_0^2 \tau_r \bar{\rho}}{d \mu_0}, \quad (12)$$

which we will show below can be understood as an equation of state in the weak sense. Two alternative formulations of this result can be given: (i) The active contribution $p_0 = (\bar{\rho}/d) f_0 \ell_p$ can be rewritten as a dissipation per area, where $f_0 \equiv v_0/\mu_0$

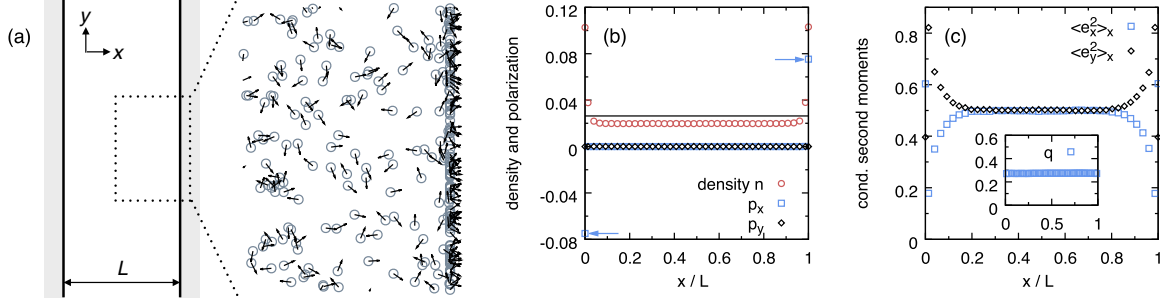


FIG. 1. Channel of width L with hard walls in x direction and periodic boundaries in y direction. (a) Sketch of channel and snapshot of particles close to one wall for reduced inverse channel width $\nu = v_0\tau_r/L = 0.5$, where arrows indicate the orientation. Note the adsorbed layer at the wall. (b) Density profile and spatially resolved average orientations for $\nu = 0.2$. Shown is the number of particles $n(x) \propto \rho(x)$ in uniformly spaced bins. The dashed line indicates the average density. The orientation (p_x and p_y) is zero everywhere except exactly at the walls (arrows). (c) Conditional second moments $\langle e_x^2 \rangle_x$ (\square) and $\langle e_y^2 \rangle_x$ (\diamond) for $\nu = 0.5$. The inset shows that $q(x) = q$ is constant away from the walls.

is an effective active force. (ii) The diffusion coefficient of noninteracting ABPs is enhanced by the active contribution $D_a = v_0^2\tau_r/d$ [37]. Employing the Einstein relation, one thus finds an ideal gas law $p_{\text{wall}} = \bar{\rho}T_{\text{eff}}$ with effective temperature $T_{\text{eff}} = T + D_a/\mu_0$.

III. LOCAL PRESSURE

To demonstrate that the concept of a local pressure is still useful even for active particles, we abandon the closed system and consider an infinite channel of width L bounded by two walls [see Fig. 1(a)]. To recover the limit of a large system, we formally let $L \rightarrow \infty$. Note that all numerical data presented in the following correspond to $T = 0$, while for the analytical calculations we retain a finite temperature T . In Fig. 1(a), we clearly see that particles adsorb at the wall with particle orientations pointing towards the wall. The system is translationally invariant so that $\psi(x, \varphi, t)$ is independent of y and Eq. (6) simplifies to

$$\partial_t \psi = -\nabla_x (v_0 e_x + \mu_0 F_x^s - \mu_0 T \nabla_x) \psi + \frac{1}{\tau_r} \partial_\varphi^2 \psi. \quad (13)$$

Integration over φ yields a steady-state condition that corresponds to the current being zero,

$$v_0 p_x + \mu_0 \rho F_x^s - \mu_0 \nabla_x (\rho T) = 0, \quad (14)$$

where $p_x(x)$ is the x component of the polarization $\mathbf{p}(x)$ (there should be no confusion with the pressure). We see immediately that for $T = 0$ then $\mathbf{p} = 0$ except at the walls, as shown numerically in Fig. 1(b). To the extent that ρT is a local pressure, this equation corresponds to hydrostatic equilibrium ($\rho \mathbf{f} - \nabla p_{\text{loc}} = 0$, where \mathbf{f} is a one-body force per particle). Here, the external forces and the internal polarization density provide the relevant one-body forces, which are balanced by pressure gradients [4, 38]. We stress that this equation does not depend on the dynamics of the orientation \mathbf{e} , it is valid even if torques are present. This is our first piece of evidence that ρT might serve as local pressure even for ABPs.

In addition, multiplying by e_x in Eq. (13) and then integrating over the orientation, we have (in steady state)

$$\nabla_x (v_0 q + \mu_0 F_x^s p_x - \mu_0 T \nabla_x p_x) + p_x / \tau_r = 0, \quad (15)$$

where

$$q(x) \equiv \int_0^{2\pi} d\varphi e_x^2 \psi(x, \varphi) \quad (16)$$

is the second moment. For $T = 0$, we have from Eq. (14) that $p_x = 0$ except at the walls. Hence, from Eq. (15), $q = q(x)$ is constant everywhere except at the walls [inset to Fig. 1(c)]. Figure 1(c) shows the conditional second moments $\langle e_x^2 \rangle_x = q/\rho(x)$ and $\langle e_y^2 \rangle_x = 1 - \langle e_x^2 \rangle_x$. In the center of the channel, we find $\langle e_x^2 \rangle_x \simeq \frac{1}{2}$ corresponding to uniformly distributed orientations since

$$\int_0^{2\pi} d\varphi \cos^2 \varphi P(\varphi) = \frac{1}{2} \quad (17)$$

with $P(\varphi) = (2\pi)^{-1}$. Approaching the walls, the distribution of e_x changes, due to the exchange of particles between bulk and the adsorbed layers.

Using Eq. (14) to eliminate the nongradient term in Eq. (15), we obtain $\rho F_x^s = \nabla_x G$ with

$$G(x) \equiv \rho T + v_0 \tau_r (p_x F_x^s + v_0 q / \mu_0 - T \nabla_x p_x), \quad (18)$$

which takes the role of an effective potential. This relationship enables two useful calculations. First, following Solon *et al.* [5], we integrate from the center of the channel ($x = L/2$) to a point outside the system ($x \rightarrow \infty$). The mechanical pressure on the right wall then reads as

$$\begin{aligned} p_{\text{wall}} &= - \int_{L/2}^{\infty} dx \rho F_x^s = G(L/2) \\ &= \rho(L/2)T + \frac{v_0^2 \tau_r}{\mu_0} q(L/2), \end{aligned} \quad (19)$$

where we used $G \rightarrow 0$ as $x \rightarrow \infty$ and $p_x(L/2) = 0$ (by symmetry). This result relates the wall pressure to a local measurement of ρ and q , which thus fulfills our weak formulation for an equation of state. Equation (19) still depends on the distance from the wall. For a wide channel, we let $L \rightarrow \infty$ with $\rho(L/2) = \bar{\rho}$ and $q(L/2) = \bar{q}/2$ [cf. Eq. (17)], which leads to the same pressure Eq. (12) as in a large closed system [2–7]. As discussed in Ref. [6], the derivation is valid only if the walls do not exert torques on the particles, in which case the wall pressure would still depend on properties of the boundary [12]. (That is, we require that \mathbf{e}_i undergoes free

rotational diffusion for all particles, even if they are in contact with the wall.) Our discussion highlights that this result hinges on a force density that can be written as a gradient, viz., the existence of a potential (18).

However, note that we can relate the wall pressure not only to the center of the channel, but also to the density at the walls. Consider a hard wall for $T > 0$ and integrate $\rho F_x^s = \nabla_x G$ from $x = L/2$ to $x = L^-$ just inside the wall so that the force $F_x^s(L^-) = 0$ vanishes and hence $G(L/2) = G(L^-)$. At the wall we have the boundary condition $v_0 q / \mu_0 = T \nabla_x p_x$ (see Appendix A). Inserting $G(L/2) = G(L^-) = \rho(L^-)T$ into Eq. (19), we thus arrive at

$$p_{\text{wall}} = (\rho T)_{\text{wall}}, \quad (20)$$

which is our second piece of evidence that ρT can be interpreted as a local pressure: the same quantity that plays the part of the local pressure in Eq. (14) also yields the mechanical pressure when evaluated at a (hard) wall. In the limit $T \rightarrow 0$, the density diverges at the wall, maintaining a finite value of $(\rho T)_{\text{wall}}$.

The third piece of evidence that $\rho(\mathbf{r})T$ is the most appropriate definition of the local pressure comes from considering a Langevin system with finite friction (for the detailed calculation, see Appendix B). In this case, one has a straightforward definition of the local pressure tensor in terms of momentum exchange with the environment of a localized subsystem: in the overdamped limit this reduces to the local pressure $\rho(\mathbf{r})T$. This result is independent of the active forces because, while the active forces do affect the velocity, they have negligible contribution to the momentum flux in the overdamped limit. Equation (14) also has a natural interpretation as force balance (hydrostatic equilibrium) in this case. Note that this result for the local pressure requires that we take the overdamped limit with a fixed value of the orientational diffusion time τ_r . If one alternatively takes $\tau_r \rightarrow 0$ (with fixed $D_a = v_0^2 \tau_r / d$) before taking the overdamped limit, the system becomes microscopically reversible and one recovers simple (passive) diffusion with effective temperature $T_{\text{eff}} = T + D_a / \mu_0$ (see Fig. 2). While this is the same effective temperature as in the large closed system [Eq. (12)], the active and passive systems differ qualitatively: in the passive system, there are no adsorbed layers at the walls of the system, and the (local) pressure is equal to the wall pressure ρT_{eff} .

IV. PRESSURE IN FINITE SYSTEMS

A. Mechanical pressure

We now explicitly calculate the mechanical pressure exerted by the active particles onto the walls for any value of the channel width L . The geometry of the channel affects the system through a single dimensionless control parameter, the reduced inverse channel width $\nu \equiv \ell_p / L$. For clarity, we also take $T = 0$, so particles move only in response to active forces. We recall Fig. 1(a), which shows that particles in the channel form an adsorbed layer at the boundaries, and that the particles in the layer have orientations pointing towards the wall. The nonuniformity of the density is also shown in Fig. 1(b). Although the system is quite simple, a full analytical

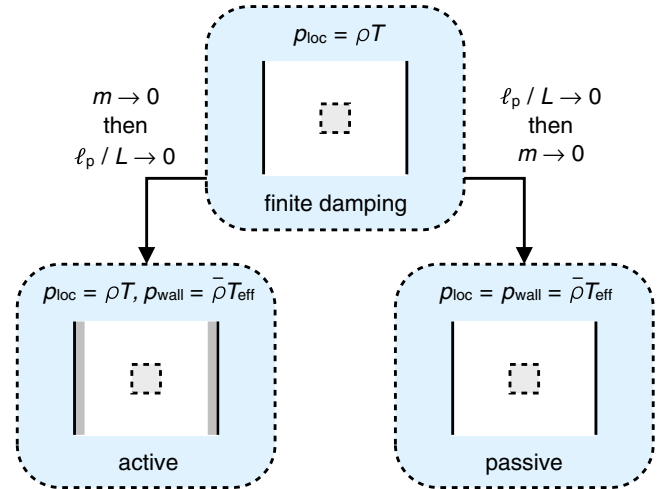


FIG. 2. The order of limits matters. Starting from dynamics with finite damping and finite speed $v_0 > 0$, the overdamped limit $m \rightarrow 0$ (with mass m) and the limit $\ell_p / L \rightarrow 0$ do not commute. Taking the overdamped limit first (left) leads to ABPs in a large system, for which there is an adsorbed layer (dark stripes) and thus local and wall pressure are different. Taking the overdamped limit last (right), one obtains a passive system with uniform density, in which local and wall pressure agree (with effective temperature T_{eff}). Note that the wall pressures for both the active and passive overdamped system coincide.

solution for the density profile is already out of reach [21,22] and we solve the equations of motion numerically.

For $T = 0$, we make the ansatz

$$\psi(x, \varphi) = \psi_0(x, \varphi) + \frac{N n_b}{L_y} [\delta(x - L) P(\varphi) + \delta(x) P(-\varphi)], \quad (21)$$

where $\psi_0(x, \varphi)$ is a smooth function and the Dirac delta functions account for the adsorbed layers. The fraction of particles in each adsorbed layer is n_b and $P(\varphi)$ is normalized as $\int d\varphi P(\varphi) = 1$. Figure 1(b) shows that the polarization $\mathbf{p}(\mathbf{r})$ is zero everywhere except for the adsorbed layers, as predicted by Eq. (14), since $T = 0$. The average orientation of a particle within the layer at $x = L$ is $\langle e_x \rangle_L = \int d\varphi \cos \varphi P(\varphi)$. For the layer at $x = 0$, then $\langle e_x \rangle_0 = -\langle e_x \rangle_L$.

The pressure on the walls can be analyzed in terms of the adsorbed layers. Each particle in such a layer exerts a force $f = f_0 e_x = (v_0 / \mu_0) e_x$ on the wall so the pressure is

$$p_{\text{wall}} = \langle f \rangle = \frac{v_0 \bar{\rho}}{\mu_0} n_b L \langle e_x \rangle_L \quad (22)$$

employing the distribution (21). Numerically, for the moments we find $\langle e_x \rangle_L \simeq 0.73$ and $\langle e_x^2 \rangle_L = \int d\varphi \cos^2 \varphi P(\varphi) \simeq 0.60$, independent of ν .

The number of particles trapped at each wall can be determined from a two-state model, where a particle is adsorbed with rate $k_{1 \rightarrow 0} \sim v_0 / L$ and goes back to the bulk with rate $k_{0 \rightarrow 1} \sim 1 / \tau_r$. Balancing adsorption and desorption rates, $n_b k_{0 \rightarrow 1} = (n_\infty - n_b) k_{1 \rightarrow 0}$, we obtain $n_b(\nu) = n_\infty / (1 + \alpha / \nu)$, the agreement of which with the numerical results is excellent [see Fig. 3(a)], with fitted $n_\infty \simeq 0.41$ and

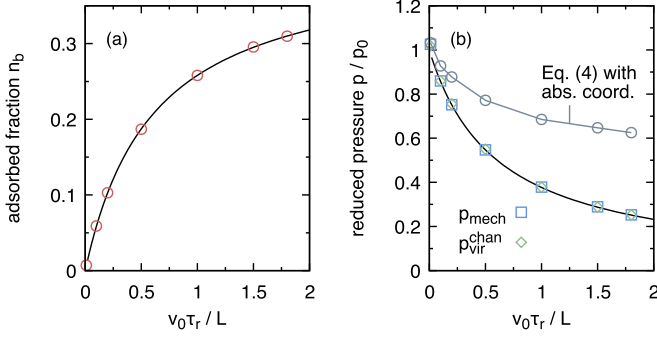


FIG. 3. (a) Fraction n_b of particles adsorbed at each wall (i.e., their orientations point into the wall) as a function of reduced inverse channel width. (b) Reduced pressure. Shown are the numerical results (symbols) for the mechanical pressure [Eq. (22)] and the virial pressure [Eq. (26)] together with the analytical prediction [Eq. (23), line], which show excellent agreement. In contrast, evaluating the virial pressure from Eq. (4) employing absolute positions overestimates the mechanical pressure (see Sec. IV B). In all cases, the ratio p/p_0 approaches unity for infinite systems $v \rightarrow 0$.

$\alpha \simeq 0.60$.¹ Substituting these results in Eq. (22), we obtain

$$p_{\text{wall}}(v) = \frac{p_0}{1 + v/\alpha} \quad (23)$$

with p_0 as defined in Eq. (12), which is recovered in the large-system limit $v = \ell_p/L \rightarrow 0$ corresponding to an effectively thermalized gas with a pressure p_0 . As expected, the pressure in a wide infinite channel is the same as that of a large closed system. While the reduction of mechanical pressure for narrow channels has been noted in numerical studies [39,40], its connection to correlations has not been discussed so far.

B. Periodic boundaries and the winding number

Before discussing the correlations, we go back to the virial pressure and derive the analog of Eq. (4) for the channel. To this end, we multiply Eq. (13) by x^2 . On integration by parts (twice) with respect to x , boundary terms vanish due to confinement of the system, and in a steady state we have

$$0 = 2\mu_0 \langle x F_x^s \rangle + 2v_0 \langle x e_x \rangle + 2\mu_0 T. \quad (24)$$

One identifies $N \langle x F_x^s \rangle = -p_{\text{wall}} L L_y$, where p_{wall} is the mechanical pressure, leading to

$$p_{\text{wall}} = \bar{\rho} T + \frac{v_0 \bar{\rho}}{\mu_0} \langle x e_x \rangle. \quad (25)$$

Due to the translational invariance, the correlations $\langle y e_y \rangle \propto \langle e_y \rangle = 0$ vanish, leading to a virial pressure

$$p_{\text{vir}}^{\text{chan}} \equiv \bar{\rho} T + \frac{v_0 \bar{\rho}}{(d-1)\mu_0} \langle \mathbf{e} \cdot \mathbf{r} \rangle, \quad (26)$$

with $p_{\text{wall}} = p_{\text{vir}}^{\text{chan}}$ for the infinite channel. It differs from Eq. (4) for the closed system through the factor of $d-1$ on

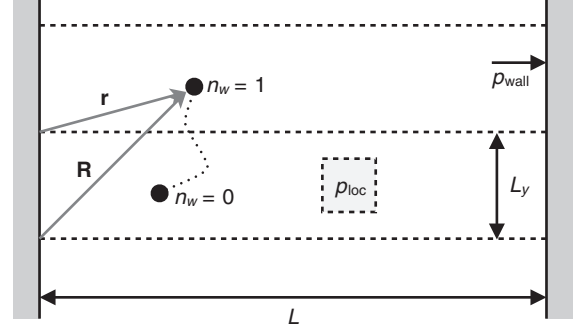


FIG. 4. Channel bounded by two hard walls. We consider a box with dimensions $L \times L_y$ bounded by two hard walls and periodic boundary conditions in y direction. The two pressures are indicated, the mechanical pressure p_{wall} exerted on the walls and the local pressure p_{loc} defined for a small subsystem away from the walls. Sketched is the trajectory of a single particle crossing the boundary of the box. Its position can thus be described by either \mathbf{r} within the periodic box or the absolute position $\mathbf{R} = n_w L_y \mathbf{e}_y + \mathbf{r}$ with winding number n_w .

the right hand side. We have performed numerical simulations to obtain the mechanical pressure p_{wall} (from the forces of adsorbed particles) and to evaluate Eq. (26) by calculating the correlations from all particles. The result is plotted in Fig. 3(b) as a function of v , showing that both pressures indeed agree.

Since the mechanical pressure is the same for the closed system and the channel, the difference between Eqs. (4) and (26) means that the correlation function $\langle \mathbf{e} \cdot \mathbf{r} \rangle$ must be different in these two geometries. Some care is required in analyzing this correlation function, due to its dependence on boundary conditions: this fact is intrinsically related to the dependence of the active pressure on particle ordering near the boundaries (walls) of the system. To illustrate this, note that our simulations employ a finite box with dimensions $L \times L_y$. To simulate the infinite channel, we introduce periodic boundaries in y direction (see Fig. 4). When calculating the correlations $\langle \mathbf{e} \cdot \mathbf{r} \rangle$ numerically, we take the position \mathbf{r} as the *periodic* position, *within* the simulation box. This is the typical situation for calculating pressures in passive simulations. It ensures that the pressure can be determined from configurations alone and thus is a local observable.

In contrast, it has previously been argued that one should evaluate $\langle \mathbf{e} \cdot \mathbf{r} \rangle$ by taking $\mathbf{r} \rightarrow \mathbf{R}$ as the *absolute* position $\mathbf{R} = n_w L_y \mathbf{e}_y + \mathbf{r}$, which takes into account the crossing of periodic boundaries [2,7] (see Fig. 4). Practically, this means that one has to introduce a winding number n_w counting the number of periodic boxes a particle has traversed, analogous to the calculation of, e.g., the mean-square displacement. The winding number clearly is not a local observable (it depends on the history of the particle). Therefore, even if the pressure of the system can be written in terms of the correlation function $\langle \mathbf{e} \cdot \mathbf{r} \rangle$ that is evaluated in this way, this does not constitute an equation of state even in the weak sense since the estimate for the pressure depends on the histories of all particles in the system. In Fig. 3(b), we have plotted the pressure employing Eq. (4) with absolute positions along the channel (including winding numbers). As $\ell_p/L \rightarrow 0$, the correct result for a large system

¹If a two-state description held exactly, one would have $n_\infty = 0.5$, so this simple description is not perfect, but the good fit in Fig. 3(a) indicates that it does capture the essential physics.

is recovered. However, for finite channel width L employing the absolute positions overestimates the mechanical pressure.

Note also that while Eq. (26) generalizes Eq. (4) to the channel geometry, there is no direct generalization to a fully periodic system without introducing winding numbers or other history-dependent terms. This is in contrast to the equilibrium virial formula for the pressure in systems of interacting particles, where the analog of the $\langle \mathbf{e} \cdot \mathbf{r} \rangle$ term depends only on separations between pairs of particles, and is easily estimated from simulations of periodic systems.

C. Active pressure is a boundary effect

We finally stress that the active pressure is controlled entirely by boundary effects. Evaluating the correlations $\langle \mathbf{e} \cdot \mathbf{r} \rangle$ in a small volume B away from the boundaries leads to

$$\langle \mathbf{e} \cdot \mathbf{r} \rangle_B = \int_B d\mathbf{r} \, \mathbf{p}(\mathbf{r}) \cdot \mathbf{r} = 0 \quad (27)$$

since $\mathbf{p} = 0$ [cf. Fig. 1(b)]. Hence, in agreement with the local pressure being independent of the active forces, ABPs do not exert a pressure by themselves but only due to their accumulation at walls caused by the directed motion. This means that the *bulk pressure* (that is, the local pressure far from any boundaries) is equal to $\bar{\rho}T$ and vanishes in the limit $T \rightarrow 0$, for which all particle motion comes from active forces. While this might seem surprising, the reason is that the active forces do not contribute to the momentum flux (see Appendix B).

D. Obstacles

Finally, we discuss what happens when the environment in which the particles move is changed via the introduction of a second length scale. To this end, we place hard circular obstacles with radius R along the center of the infinite channel [see Fig. 5(a) for a snapshot]. The distance between obstacles is L_y . We still employ periodic boundary conditions for the y direction with one obstacle per box and adjust L_y so that the global density $\bar{\rho}$ remains unchanged. Hence, we now have two reduced lengths, $\ell_p/L = \nu$ as before and R/L .

Figure 5(a) shows that the particles accumulate at the obstacle, as expected. In Fig. 5(b), we plot the reduced mechanical pressure p_{wall}/p_0 exerted onto the two outer walls as a function of radius R/L for two values of ν . It shows that the presence of the obstacle reduces the forces on the outer walls. We have also calculated the virial pressure $p_{\text{vir}}^{\text{chan}}$ [Eq. (26)], which for small ν deviates from the mechanical pressure. Hence, in the presence of internal walls, the correlations are not sufficient anymore to capture the mechanical pressure.

We now generalize the approach of Sec. III. The system is no longer translationally invariant. However, all quantities are periodic functions with respect to the y coordinate. The mechanical pressure [cf. Eq. (19)] reads as

$$p_{\text{wall}} = -\frac{1}{L_y} \int_0^{L_y} dy \int_x^\infty dx \, \rho F_x^s, \quad (28)$$

where the lower limit of integration is now a plane $x = X$ outside the obstacle $(L/2 + R) < X < L$. While Eq. (14) still holds, the force density now reads as $\rho F_x^s = \nabla_x G + \nabla_y G_y$

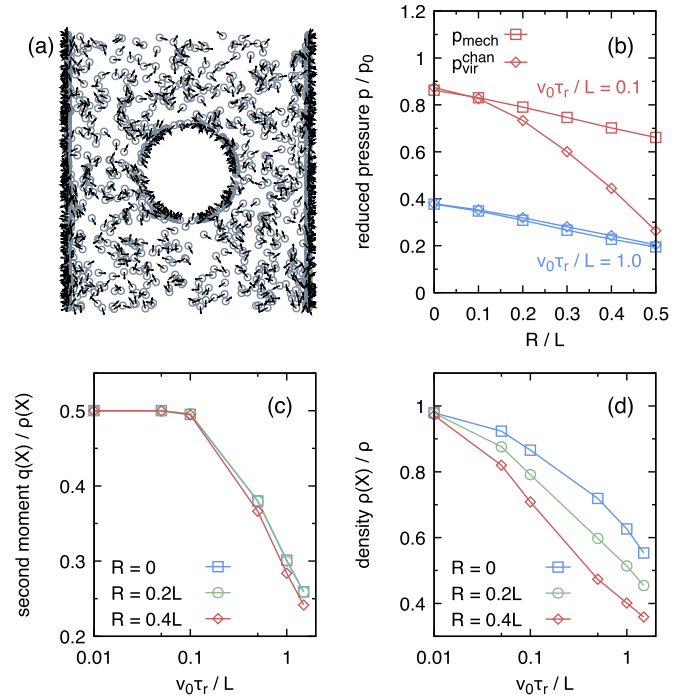


FIG. 5. Channel with obstacles. (a) Snapshot for $\nu = 0.5$ and obstacle radius $R/L = 0.2$. (b) Reduced pressure for two values of ν as a function of obstacle radius R/L . (c) Conditional second moment for a plane $x = X$ close to the walls. (d) Reduced density $\rho(X)/\bar{\rho}$.

with potential $G = G(\mathbf{r})$ similar to that in Eq. (18) and an additional potential term $G_y(\mathbf{r})$. The latter term does not contribute to p_{wall} due to periodicity of the y integral in Eq. (28). Using again that $G \rightarrow 0$ as $x \rightarrow \infty$, we obtain

$$p_{\text{wall}} = \frac{1}{L_y} \int_0^{L_y} dy \, G(X, y). \quad (29)$$

For $T = 0$ we numerically find $p_x = 0$, away from the walls.² Hence, the mechanical pressure reduces to

$$p_{\text{wall}} = \frac{v_0^2 \tau_r}{\mu_0} \bar{q}(X), \quad (30)$$

where the second moment $\bar{q}(X)$ is evaluated at the plane $x = X$, and is averaged over the y coordinate. Figure 5(c) shows the behavior of $\bar{q}(X)/\rho(X)$ for a plane close to the walls as a function of $\nu = \ell_p/L$ for different obstacle radii. The ratio approaches $\bar{q}(X)/\rho(X) \rightarrow \frac{1}{2}$. In Fig. 5(d), the density $\rho(X)/\bar{\rho}$ is plotted, which shows that in the chosen plane the density also approaches the bulk density. Both figures show that in the limit of a large system with fixed R/L the same wall pressure Eq. (12) is recovered as in the closed system and the infinite channel without obstacles. However, the virial formula (26) does not coincide with the mechanical pressure, due to the presence of the internal walls.

²In contrast to the translationally invariant channel where $p_x = 0$ follows from Eq. (15), deriving the equivalent result in the presence of the obstacle requires an assumption that there are no persistent currents in the steady state of the system. This condition is in fact satisfied within our numerics, so $p_x = 0$.

V. DISCUSSION

Suppose we want to know the pressure of, say, liquid argon at a given temperature. We can perform a computer simulation employing the Lennard-Jones pair potential with a fixed number of particles and fixed box size. An instantaneous pressure is calculated from the particle positions and averaged over many configurations sampled at equilibrium. The larger the system, the fewer configurations are needed to converge the numerical estimate for the pressure. Periodic boundaries are helpful here, in that they enable accurate estimates of bulk quantities from simulations of finite systems, as long as the simulated system is large (in comparison with microscopic correlation lengths). Moreover, if a very large system is considered, the pressure can be measured by observing a finite subsystem within it, and the result is independent of the subsystem chosen. This is true even if the system is inhomogeneous, for example, if it contains liquid and vapor in coexistence.

In contrast, the mechanical pressure of active particles is intrinsically wound up with the layers of particles which form at the boundary of the system. This observation prevents estimation of the mechanical pressure in terms of state variables within periodic systems, even for the simplest case of noninteracting active Brownian particles (see Sec. IV B). To the extent that a local pressure can be defined (either in periodic systems or in finite subsystems far from walls), it is equal to ρT , as shown here, and therefore differs from the mechanical pressure. In that strict sense, an equation of state does not exist for active Brownian particles. A weaker formulation [cf. Eq. (19)] still holds for torque-free spherical particles [5], which relates the mechanical pressure to the second moment q of orientations. It explicitly involves walls and only in the limit $\ell_p/L \rightarrow 0$ of a large separation of these walls does q become a true bulk quantity. The physical picture is that in this limit the single adsorption events onto walls become uncorrelated and the active forces thus contribute uncorrelated noise that can be described by an elevated effective temperature.

Since estimators involving winding numbers can reproduce the mechanical pressure for large systems, it might be argued that the requirement to track such history-dependent quantities is an essential price to pay for estimating pressure out of equilibrium. We note, however, that such an approach does not capture the properties of finite systems (Fig. 3). Moreover, if systems are inhomogeneous (for example, due to motility-induced phase separation), the properties of numerical estimators involving winding numbers can be extremely poor since convergence of averaged values requires that typical particles spend significant time in both dense and sparse phases, during the simulated trajectories [8]. This fact again emphasizes that the winding number is not a local observable, and that approaches based on such observables cannot be used to characterize the local pressure or stresses in the fluid. This last observation is important since a practical motivation for defining the pressure is the derivation of hydrodynamic equations (in the spirit of Navier-Stokes), in which fluid flow on macroscopic scales depends on pressure gradients, as well as other macroscopic properties such as viscosity. A local definition of pressure is essential for such an approach: this motivates our interpretation of equations such as (15) in terms of hydrostatic equilibrium (local force balance).

VI. CONCLUSIONS

In this article, we have argued that the local pressure of ideal active Brownian particles should be identified as $\rho(\mathbf{r})T$. This differs from the mechanical pressure exerted on walls of the system because the walls induce changes in local density via the formation of an adsorbed layer of particles. For hard walls, the mechanical pressure is given by $(\rho T)_{\text{wall}}$, which lends extra support to our interpretation. The extension of these results to ABPs that interact by a two-body potential is straightforward and will be discussed in a future publication. Our results are an important step towards a better theoretical understanding of pressure and forces on immersed bodies [40–43], which will be crucial for future application of active particles in, e.g., self-assembly. It would also be useful to connect this work with recently proposed mappings between ABPs and effective equilibrium systems [44–46], in which the pressure necessarily is local.

Two questions that remain outstanding are (i) whether (and how) these results can be related to nonequilibrium analogs of the “thermodynamic” pressure defined in terms of large deviations of the density (on the hydrodynamic scale); and (ii) can the arguments presented here be extended to systems where the orientational evolution of the particles is no longer independent of the particle positions? Examples of this latter situation include the presence of external torques (e.g., favoring alignment at walls), or torques arising from interactions between particles. Finally, it is not clear to what extent we can expect a general hydrodynamic description of active fluids in terms of local pressure, density, and velocity, but we feel that identifying cases in which such a description is possible is a key goal in this area [47,48]. An appropriate definition of the local pressure is obviously vital if this is to be achieved.

ACKNOWLEDGMENTS

We thank H. Löwen, R. Winkler, G. Szamel, and J. Tailleur for helpful discussions and comments. T.S. gratefully acknowledges financial support by the DFG within priority program SPP 1726 (Grant No. SP 1382/3-1).

APPENDIX A: BOUNDARY CONDITION AT A HARD WALL

We derive the boundary condition of the active fluid at a hard wall by taking the limit of a “soft” wall, for which \mathbf{F}^s is a finite x -dependent force. We consider a single wall at $x = 0$, so that the force \mathbf{F}^s lies in the positive x direction for $x < 0$, with $\mathbf{F}^s = 0$ for $x > 0$. The wall confines the system so $\psi \rightarrow 0$ as $x \rightarrow -\infty$.

Take $X > 0$ and consider the time derivative

$$\int_{-\infty}^X dx \int dy \partial_t \psi = 0 \quad (\text{A1})$$

of the number of particles with orientation φ and $x < X$, which vanishes in the steady state. Also, translational invariance along the wall means that $\psi = \psi(x, \varphi)$, so the y integral in (A1) corresponds simply to multiplication by a constant. Using

Eq. (13) and performing the integration over x , we have

$$0 = -v_0 e_x \psi(X, \phi) + \mu_0 T \nabla_x \psi(X, \phi) + \frac{1}{\tau_r} \int_{-\infty}^X dx \partial_\phi^2 \psi(x, \phi), \quad (\text{A2})$$

where we used $\mathbf{F}^s(X) = 0$. Now, take the hard wall limit, in which case $\psi = 0$ for all $x < 0$. Then, take $X \rightarrow 0$ (from above). For $T > 0$ then ψ is a smooth function so the integrand in the last term is finite in the limit, and the support of the integral goes to zero. Hence, for all ϕ

$$v_0 e_x \psi(0, \phi) = \mu_0 T (\nabla_x \psi)_{x=0}, \quad (\text{A3})$$

which is the boundary condition at the hard wall. Multiplying by e_x and integrating over ϕ yields the boundary condition $v_0 q = \mu_0 T \nabla_x p_x$.

APPENDIX B: FINITE DAMPING

1. Momentum transfer

We consider particles with finite mass m that move with velocity $\mathbf{v}_i = \dot{\mathbf{r}}_i$, with

$$m \dot{\mathbf{v}}_i = \mathbf{F}_i - (\mathbf{v}_i / \mu_0) \quad (\text{B1})$$

and \mathbf{F}_i given by Eq. (1). We identify $(1/\mu_0)$ as a friction (damping) coefficient. If we take $m \rightarrow 0$, then we recover the overdamped dynamics considered in the main text.

To define a local pressure, we consider a subsystem B of a large system with its center at \mathbf{r}_0 (cf. Fig. 4). There are no walls inside the subsystem and particles can move into and out of the subsystem. The total momentum inside B can change either due to “direct” forces from outside the subsystem, or due to particles carried into (or out of) the subsystem by particles crossing the boundary (i.e., momentum flux). The direct contribution to the pressure is

$$p_{\text{ext}} = \frac{N}{A_b} \langle -\mathbf{F}_i^{\text{ext}} \cdot \mathbf{n}_b \rangle, \quad (\text{B2})$$

where $\mathbf{F}_i^{\text{ext}}$ is the force exerted on particle i by particles that are external to subsystem B , \mathbf{n}_b is normal to the boundary of B , and A_b is the length (area) of the boundary being considered.

The other contribution to the pressure is the rate of momentum transfer into the system from the outside, minus the rate of momentum transfer out of the system from the inside. These two terms are equal in magnitude and together they sum to

$$p_{\text{mom}} = m \langle \rho (v^\perp)^2 \rangle_{\text{bndy}}, \quad (\text{B3})$$

where $v^\perp \equiv \mathbf{n}_b \cdot \mathbf{v}$ is the velocity perpendicular to the boundary and the average is taken in a small region located at the boundary. This motivates the definition of a (local) momentum flux tensor $\pi^{\alpha\beta} = m \langle \rho v^\alpha v^\beta \rangle$, which can be evaluated locally. If the system is isotropic, then one has $\pi^{\alpha\beta} = p_{\text{mom}} \delta^{\alpha\beta}$ with $p_{\text{mom}} = m \langle \rho v^2 \rangle / d$.

The pressure (defined in terms of momentum exchange) for subsystem B is $p_{\text{loc}} = p_{\text{mom}} + p_{\text{ext}}$. For ideal (noninteracting) systems as defined here, we consider a subsystem far from any walls, in which case $p_{\text{ext}} \rightarrow 0$ and p_{mom} can be interpreted as the local pressure. Taking the overdamped limit $m \rightarrow 0$ at

fixed τ_r , we find (see below)

$$m \langle \rho v^\alpha v^\beta \rangle \rightarrow \rho T \delta^{\alpha\beta}, \quad (\text{B4})$$

which is the same result as one obtains from (classical) equipartition of energy at equilibrium. Hence, the local pressure is $p_{\text{loc}}(\mathbf{r}) = p_{\text{mom}}(\mathbf{r}) = \rho(\mathbf{r})T$.

On the other hand, taking the limit of small τ_r (at fixed $D_a = v_0^2 \tau_r / d$), we show in the following that all nonequilibrium aspects of the problem disappear: the active swim force behaves in the same way as an extra thermal noise the particle, and one recovers equilibrium behavior at a higher temperature $T_{\text{eff}} = T + D_a / \mu_0$.

2. Position and velocity correlations

To derive (B4), and investigate the behavior of correlations between particles' velocities and their orientations, we consider the equations of motion for a single active particle far from any walls. (To achieve this in practice, consider a periodic system in two dimensions, without any external forces acting. In a large closed system, we can assume that particles spend negligible time in contact with the walls, in which case the following results still apply.)

The Fokker-Planck equation that generalizes (6) is then

$$\partial_t \Psi = -\mathbf{v} \cdot \nabla_{\mathbf{r}} \Psi + \frac{1}{m \mu_0} \nabla_{\mathbf{v}} \cdot \left[\mathbf{v} - v_0 \mathbf{e} + \frac{T}{m} \nabla_{\mathbf{v}} \right] \Psi + (1/\tau_r) \partial_\phi^2 \Psi, \quad (\text{B5})$$

where $\Psi = \Psi(\mathbf{r}, \mathbf{v}, \phi, t)$ is the distribution function for the particle's position, velocity, and orientation, and the vector \mathbf{e} has elements $(\cos \phi, \sin \phi)$. The gradients $\nabla_{\mathbf{r}}, \nabla_{\mathbf{v}}$ act on the position and velocity coordinates, respectively. It is convenient to write $\partial_t \Psi = \mathbb{W} \Psi$ where \mathbb{W} is a second order differential operator that may be read off from (B5), and we have (formally) $\Psi(t) = e^{\mathbb{W}t} \Psi(0)$. If we also assume that Ψ is independent of position \mathbf{r} , then this property is maintained by the dynamical evolution and we can consider $\Psi = \Psi(\mathbf{v}, \mathbf{e}, t)$.

As in the Heisenberg picture of quantum mechanics, we define time-dependent operators for the velocity and orientation as $\hat{\mathbf{v}}(t) = e^{-\mathbb{W}t} \hat{\mathbf{v}} e^{\mathbb{W}t}$ and $\hat{\mathbf{e}}(t) = e^{-\mathbb{W}t} \hat{\mathbf{e}} e^{\mathbb{W}t}$. It is also convenient to define a momentum operator conjugate to the velocity $i \hat{\mathbf{P}}_v = \nabla_{\mathbf{v}}$ and its time-dependent analog $\hat{\mathbf{P}}_v(t) = e^{-\mathbb{W}t} \hat{\mathbf{P}}_v e^{\mathbb{W}t}$. Also, $i P_\phi = \partial_\phi$ with a similar time-dependent analog. Then, one has (in terms of operators)

$$\begin{aligned} \partial_t \hat{\mathbf{v}}(t) &= [-\hat{\mathbf{v}}(t) + v_0 \hat{\mathbf{e}}(t)] / (m \mu_0) - 2i T \hat{\mathbf{P}}_v(t) / (m^2 \mu_0), \\ \partial_t \hat{\mathbf{e}}(t) &= -\hat{\mathbf{e}}(t) / \tau_r + 2i \hat{p}_\phi(t) \hat{\mathbf{e}}^\perp(t) / \tau_r, \end{aligned} \quad (\text{B6})$$

where \mathbf{e}^\perp is the vector $(\sin \phi, -\cos \phi)$ which is perpendicular to \mathbf{e} . Since we have assumed that Ψ is independent of \mathbf{r} , we also have $\partial_t \hat{\mathbf{P}}_v(t) = \hat{\mathbf{P}}_v(t) / (m \mu_0)$. Expectation values in the steady state of the model are given by $\langle \hat{A} \rangle = \int d\mathbf{v} d\mathbf{e} d\mathbf{r} \hat{A} \Psi_{\text{ss}}$ where Ψ_{ss} is the steady-state solution of (B6).

With this machinery in place, standard methods allow us to write and then solve equations of motion for correlation functions: for example, considering vector components of the

velocity, one has

$$\partial_t \langle v_t^\alpha v_{t'}^\beta \rangle = [-\langle v_t^\alpha v_{t'}^\beta \rangle + v_0 \langle e_t^\alpha v_{t'}^\beta \rangle] / (m\mu_0) - 2iT \langle P_{v,t}^\alpha v_{t'}^\beta \rangle / (m^2\mu_0). \quad (\text{B7})$$

By considering a similar expression for $\partial_{t'} \langle v_t^\alpha P_{v,t'}^\beta \rangle$, one obtains

$$i \langle v_t^\alpha P_{v,t'}^\beta \rangle = -\delta^{\alpha\beta} \Theta(t - t') e^{-(t-t')/(m\mu_0)}, \quad (\text{B8})$$

where $\Theta(t - t')$ is the Heaviside (step) function, and we used $\langle e_t^\alpha P_{v,t'}^\beta \rangle = 0$ and $\langle P_{v,t}^\alpha P_{v,t'}^\beta \rangle = 0$, which both follow from the equation of motion for $\hat{\mathbf{P}}_v(t)$.

Considering next $\partial_t \langle e_t^\alpha v_{t'}^\beta \rangle$, one has that for $t > t'$

$$\langle e_t^\alpha v_{t'}^\beta \rangle = \langle e_{t'}^\alpha v_{t'}^\beta \rangle e^{-(t-t')/\tau_r}. \quad (\text{B9})$$

To fix the prefactor, we use time translation invariance of the steady state, so that $(\partial_t + \partial_{t'}) \langle e_t^\alpha v_{t'}^\beta \rangle = 0$. Evaluating this expression as $t \rightarrow t'$, one obtains the value of $\langle e_{t'}^\alpha v_{t'}^\beta \rangle$ and hence

$$\langle e_{t'}^\alpha v_{t'}^\beta \rangle = \delta^{\alpha\beta} \frac{v_0 \tau_r}{d(\tau_r + m\mu_0)} e^{-(t-t')/\tau_r}, \quad t > t' \quad (\text{B10})$$

where we used $\langle e_t^\alpha e_t^\beta \rangle = \delta^{\alpha\beta}/d$ since \mathbf{e} is a randomly distributed unit vector. Note that in the overdamped limit $m \rightarrow 0$, then $\langle \mathbf{e}_t \cdot \mathbf{v}_t \rangle \rightarrow v_0$, consistent with the known behavior of ABPs.

Finally, returning to (B7), assuming $t > t'$ and using (B8) and (B10), we obtain a first-order differential equation for $\langle v_t^\alpha v_{t'}^\beta \rangle$ that can be solved using an integrating factor, yielding

$$\langle v_t^\alpha v_{t'}^\beta \rangle = C^{\alpha\beta} e^{-(t-t')/(m\mu_0)} + \delta^{\alpha\beta} \frac{v_0^2 \tau_r^2}{d[\tau_r^2 - (m\mu_0)^2]} e^{-(t-t')/\tau_r}, \quad (\text{B11})$$

where the $C^{\alpha\beta}$ are constants of integration that can be fixed using time translation invariance of the steady state, which implies $(\partial_t + \partial_{t'}) \langle v_t^\alpha v_{t'}^\beta \rangle = 0$. Hence,

$$\begin{aligned} \langle v_t^\alpha v_{t'}^\beta \rangle &= \delta^{\alpha\beta} \frac{v_0^2 \tau_r^2}{d[\tau_r^2 - (m\mu_0)^2]} e^{-|t-t'|/\tau_r} \\ &+ \delta^{\alpha\beta} \left[\frac{T}{m} - \frac{m\mu_0 v_0^2 \tau_r}{d[\tau_r^2 - (m\mu_0)^2]} \right] e^{-|t-t'|/(m\mu_0)}. \end{aligned} \quad (\text{B12})$$

The structure in this correlation function arises from the coupling of the velocity to the orientation. Note that there is no divergence as $\tau_r \rightarrow m\mu_0$ because the singular contributions from the two terms cancel each other. For active Brownian particles, we require the overdamped limit ($m \rightarrow 0$), in which case this expression simplifies, leading to a Dirac delta function that encapsulates the effect of the thermal noise, and a regular term that describes the persistent motion of the particle due to the active forces. Setting $t = t'$ and taking $m \rightarrow 0$, one also obtains $m \langle v_t^\alpha v_t^\beta \rangle \rightarrow T \delta^{\alpha\beta}$ as asserted above. That is, the momentum flux tensor is isotropic and consistent with a local pressure ρT .

For completeness, note that by considering $\partial_{t'} \langle e_t v_{t'} \rangle$, one finds that for $t' > t$,

$$\begin{aligned} \langle e_t v_{t'} \rangle &= \delta^{\alpha\beta} \frac{v_0 \tau_r}{d(\tau_r - m\mu_0)} e^{-(t'-t)/\tau_r} \\ &+ \delta^{\alpha\beta} \frac{2m\mu_0 v_0 \tau_r}{d[(m\mu_0)^2 - \tau_r^2]} e^{-(t'-t)/(m\mu_0)}, \end{aligned} \quad (\text{B13})$$

which complements (B10). It is not immediately apparent from these expressions, but we note that this correlation function is continuous at $t = t'$, and there is no divergence as $\tau_r \rightarrow m\mu_0$ because the singular contributions from the two terms cancel each other, as was the case for $\langle v_t v_{t'} \rangle$.

3. Order of limits

Finally, it is instructive to consider the limit $\tau_r \rightarrow 0$ (holding $D_a = v_0^2 \tau_r/d$ constant), in which case it may be verified that the orientation \mathbf{e} acts as a Brownian noise that modifies the effective temperature of the system. In particular, $\langle v_0 e_t^\alpha v_0 e_t^\beta \rangle \rightarrow \delta^{\alpha\beta} D_a \delta(t - t')$ means that $v_0 \mathbf{e}$ acts in the limit as a white noise, and $\langle v_t^\alpha v_0 e_{t'}^\beta \rangle \rightarrow \delta^{\alpha\beta} \Theta(t - t') \frac{2D_a}{m\mu_0} e^{-(t-t')/(m\mu_0)}$, as expected for the correlation between a velocity and a noise force. But, we emphasize that active Brownian particles do *not* under any circumstances reduce to this passive system because the ABP model is obtained by taking $m \rightarrow 0$ before any limit of small τ_r . These two limits do not at all commute, as may be easily seen from the local pressure, which is ρT for ABPs but is equal to ρT_{eff} for the effective passive case. Also, the adsorbed layer of particles at the wall is present for ABPs {with local density $\bar{\rho}[1 + D_a/(\mu_0 T)]$, from Eq. (20)}, but there is no such layer for passive particles.

-
- [1] D. Chandler, *Introduction to Modern Statistical Mechanics* (Oxford University Press, Oxford, 1987).
 - [2] S. C. Takatori, W. Yan, and J. F. Brady, *Phys. Rev. Lett.* **113**, 028103 (2014).
 - [3] S. C. Takatori and J. F. Brady, *Soft Matter* **10**, 9433 (2014).
 - [4] W. Yan and J. F. Brady, *Soft Matter* **11**, 6235 (2015).
 - [5] A. P. Solon, J. Stenhammar, R. Wittkowski, M. Kardar, Y. Kafri, M. E. Cates, and J. Tailleur, *Phys. Rev. Lett.* **114**, 198301 (2015).
 - [6] A. P. Solon, Y. Fily, A. Baskaran, M. E. Cates, Y. Kafri, M. Kardar, and J. Tailleur, *Nat. Phys.* **11**, 673 (2015).
 - [7] R. G. Winkler, A. Wysocki, and G. Gompper, *Soft Matter* **11**, 6680 (2015).
 - [8] J. Bialké, J. T. Siebert, H. Löwen, and T. Speck, *Phys. Rev. Lett.* **115**, 098301 (2015).
 - [9] S. C. Takatori and J. F. Brady, *Phys. Rev. E* **91**, 032117 (2015).
 - [10] S. C. Takatori and J. F. Brady, *Soft Matter* **11**, 7920 (2015).
 - [11] U. M. B. Marconi and C. Maggi, *Soft Matter* **11**, 8768 (2015).
 - [12] M. Joyeux and E. Bertin, *Phys. Rev. E* **93**, 032605 (2016).
 - [13] Y. Fily and M. C. Marchetti, *Phys. Rev. Lett.* **108**, 235702 (2012).
 - [14] J. Palacci, S. Sacanna, A. P. Steinberg, D. J. Pine, and P. M. Chaikin, *Science* **339**, 936 (2013).

- [15] I. Buttinoni, J. Bialké, F. Kümmel, H. Löwen, C. Bechinger, and T. Speck, *Phys. Rev. Lett.* **110**, 238301 (2013).
- [16] J. Stenhammar, A. Tiribocchi, R. J. Allen, D. Marenduzzo, and M. E. Cates, *Phys. Rev. Lett.* **111**, 145702 (2013).
- [17] J. Stenhammar, D. Marenduzzo, R. J. Allen, and M. E. Cates, *Soft Matter* **10**, 1489 (2014).
- [18] J. Bialké, T. Speck, and H. Löwen, *J. Non-Cryst. Solids* **407**, 367 (2015).
- [19] M. E. Cates and J. Tailleur, *Annu. Rev. Condens. Matter Phys.* **6**, 219 (2015).
- [20] T. Speck, A. M. Menzel, J. Bialké, and H. Löwen, *J. Chem. Phys.* **142**, 224109 (2015).
- [21] C. F. Lee, *New J. Phys.* **15**, 055007 (2013).
- [22] J. Elgeti and G. Gompper, *Europhys. Lett.* **101**, 48003 (2013).
- [23] Y. Fily, A. Baskaran, and M. F. Hagan, *Phys. Rev. E* **91**, 012125 (2015).
- [24] Y. Fily, A. Baskaran, and M. F. Hagan, *Soft Matter* **10**, 5609 (2014).
- [25] S. A. Mallory, A. Šarić, C. Valeriani, and A. Cacciuto, *Phys. Rev. E* **89**, 052303 (2014).
- [26] X. Yang, M. L. Manning, and M. C. Marchetti, *Soft Matter* **10**, 6477 (2014).
- [27] M. Spellings, M. Engel, D. Klotsa, S. Sabrina, A. M. Drews, N. H. P. Nguyen, K. J. M. Bishop, and S. C. Glotzer, *Proc. Natl. Acad. Sci. USA* **112**, E4642 (2015).
- [28] F. Smallenburg and H. Löwen, *Phys. Rev. E* **92**, 032304 (2015).
- [29] A. Wysocki, J. Elgeti, and G. Gompper, *Phys. Rev. E* **91**, 050302 (2015).
- [30] N. Nikola, A. P. Solon, Y. Kafri, M. Kardar, J. Tailleur, and R. Voituriez, [arXiv:1512.05697](https://arxiv.org/abs/1512.05697).
- [31] J. Palacci, C. Cottin-Bizonne, C. Ybert, and L. Bocquet, *Phys. Rev. Lett.* **105**, 088304 (2010).
- [32] M. Enculescu and H. Stark, *Phys. Rev. Lett.* **107**, 058301 (2011).
- [33] F. Ginot, I. Theurkauff, D. Levis, C. Ybert, L. Bocquet, L. Berthier, and C. Cottin-Bizonne, *Phys. Rev. X* **5**, 011004 (2015).
- [34] G. Falasco, F. Baldovin, K. Kroy, and M. Baiesi, [arXiv:1512.01687](https://arxiv.org/abs/1512.01687).
- [35] N. Metropolis, A. W. Rosenbluth, M. N. Rosenbluth, A. H. Teller, and E. Teller, *J. Chem. Phys.* **21**, 1087 (1953).
- [36] J. Hansen and I. McDonald, *Theory of Simple Liquids*, 3rd ed. (Academic, Amsterdam, 2006).
- [37] J. R. Howse, R. A. L. Jones, A. J. Ryan, T. Gough, R. Vafabakhsh, and R. Golestanian, *Phys. Rev. Lett.* **99**, 048102 (2007).
- [38] I. R. Thompson and R. L. Jack, *Phys. Rev. E* **92**, 052115 (2015).
- [39] B. Ezhilan, R. Alonso-Matilla, and D. Saintillan, *J. Fluid Mech.* **781**, R4 (2015).
- [40] W. Yan and J. F. Brady, *J. Fluid Mech.* **785**, R1 (2015).
- [41] J. Harder, S. A. Mallory, C. Tung, C. Valeriani, and A. Cacciuto, *J. Chem. Phys.* **141**, 194901 (2014).
- [42] D. Ray, C. Reichhardt, and C. J. Olson Reichhardt, *Phys. Rev. E* **90**, 013019 (2014).
- [43] R. Ni, M. A. Cohen Stuart, and P. G. Bolhuis, *Phys. Rev. Lett.* **114**, 018302 (2015).
- [44] T. F. F. Farage, P. Krinninger, and J. M. Brader, *Phys. Rev. E* **91**, 042310 (2015).
- [45] C. Maggi, U. M. B. Marconi, N. Gnan, and R. Di Leonardo, *Sci. Rep.* **5**, 10742 (2015).
- [46] M. C. Marchetti, Y. Fily, S. Henkes, A. Patch, and D. Yllanes, *Curr. Opin. Colloid Interface Sci.* **21**, 34 (2016).
- [47] R. Wittkowski, A. Tiribocchi, J. Stenhammar, R. J. Allen, D. Marenduzzo, and M. E. Cates, *Nat. Commun.* **5**, 4351 (2014).
- [48] A. Tiribocchi, R. Wittkowski, D. Marenduzzo, and M. E. Cates, *Phys. Rev. Lett.* **115**, 188302 (2015).